Supplement of Atmos. Chem. Phys., 19, 13289–13308, 2019
https://doi.org/10.5194/acp-19-13289-2019-supplement

Supplement of

Semi-quantitative understanding of source contribution to nitrous acid (HONO) based on 1 year of continuous observation at the SORPES station in eastern China

Yuliang Liu et al.

Correspondence to: Wei Nie (niewei@nju.edu.cn) and Zheng Xu (zheng.xu@nju.edu.cn)

The strong nearly linear correlation between OH and $J(O^1D)$ was firstly proposed by Rohrer and Berresheim (2006), based on the observations in a lightly polluted site, where the reaction of HO_2 with NO contributes most of OH radicals. This relationship has been also verified by the OH campaigns in the polluted area of China, where the most striking feature is the almost equal slope of the OH-$J(O^1D)$ relation for different locations and seasons (Rohrer et al., 2014;Tan et al., 2017;Tan et al., 2018).

The coefficients **a**, **b** and **c** in Eq. (2) characterize the average conditions of OH chemistry at a specific location. As listed in Table S1, the value of coefficient **b** is mainly distributed around 1, showing that OH is strongly linearly correlated with $J(O^1D)$ in general ($r>0.85$ in different observations), which was also derived by theoretical deduction through simplifying the reaction scheme for the chemical regime, in the study of Rohrer and Berresheim (2006). It should be noted out that the term $J(O^1D)^{\mathbf{b}}$ reflects the combined effects of all photolytic processes—for example, the photolysis of ozone, NO_2, HONO, H_2O_2 and HCHO.

The pre-exponential coefficient, **a**, is thought to condense the dependences of OH on reactants (NO_x, VOCs etc). Based on the available measurements, the values of coefficient **a** do not show great differences on various spatial and temporal scales, especially in the polluted areas of China. We can make assumptions that the comprehensive impact of reactants on OH cannot compete with that of UV light to OH, and the chemical environments of OH are similar. The not significant diversity of coefficient **a** has been proved partly from observations and models in Rohrer and Berresheim (2006) and Rohrer et al. (2014).

The light-independent OH, represented by the coefficient **c**, is variable. It seems that the value of coefficient **c** in polluted areas is higher than that in clean areas, and the value of coefficient **c** in summer is higher than that in winter (Table S1), probably due to the variability of the strength of nighttime ozone reacting with biogenic or anthropogenic VOCs. It should be noted that the variance of the coefficient **c** has little effect on the calculated OH radicals under strong solar radiation.

Table S1. the summary of the coefficients **a**, **b**, **c** of Eq. (2) in different OH observation campaigns with respect to the relation between OH and $J(O^1D)$

Location		Time	**a** [10^6cm^{-3}]	**b**	**c** [10^6cm^{-3}]	Ref.
Germany (48°N , 11°E)	rural	1999-2003	2.4	0.93	0.13 ±0.01	1
Germany (54°N , 12°E)	rural	Aug 1994	3.9	0.95	0.04 ±0.01	2
Atlantic (5°N-40°S , 26°W)	marine	Oct/Nov 1996	1.4	1.3	0.20 ±0.21	3

Germany (53°N , 13°E)	rural/urban	Jul/Aug 1998	2	0.92	0.43 ±0.02	4
Crete (35°N , 25°E)	marine/rural	Aug 2001	7.2	0.68	0.01 ±0.05	5
Guangzhou, China (23.5°N, 113.0°E)	rural	Jul 2006	5.6 4.0	0.68[A] 1[B]	2.3 2.4	6
Beijing, China (39.5° N, 116.3°E)	suburban	Aug 2006	4.4 4.0	0.88[A] 1[B]	1.4 1.6	7
Wangdu, China	rural	Jun 2014	4.5	1	1	8
Beijing, China (40.4°N, 116.7° E)	suburban	Jan/Mar 2016	4.33	1	0.22	9

1: Rohrer and Berresheim (2006); 2: Holland et al. (1998); 3: Brauers et al. (2001); 4: Holland et al. (2003); 5: Berresheim et al. (2003); 6: Lu et al. (2012); 7: Lu et al. (2013); 8: Tan et al. (2017); 9: Tan et al. (2018)

A: nonlinear fit; B: linear fit.

In this study, we set a fixed value for the coefficients **a** and **b** and seasonal change values for coefficient **c** to calculate the concentration of OH radicals, based on the OH observations in the PRD and Beijing, China. To estimate the influence of the uncertainty of the coefficients in Eq. (2), we calculate the OH radicals for a certain value of $J(O^1D)$ under the permutations and combinations of different values of the coefficients, where the coefficient **a** varies from 1×10^6 cm^{-3} to 8×10^6 cm^{-3}, the coefficient **b** varies from 0.6 to 1.3, and the coefficient **c** varies from 0 to 2.5×10^6 cm^{-3}. As showed in Fig. S1(a), the errors of OH increase with the increase of $J(O^1D)$, but the ratios of error to mean value of OH radicals are in an acceptable range of 0.37-0.55.

Regarding to the effect of the uncertainty of calculated OH on the strength of missing daytime source ($P_{unknown}$), we derive $P_{unknown}$ from Eq. (10) based on the permutations and combinations of OH radicals, J(HONO), and HONO. According to the observations, the variances of OH and J(HONO) depend on $J(O^1D)$, meaning that each of these values has a lower and upper limit for a certain value of J(O1D) (Fig. S1(a) and Fig. S1(b)). And for the same reason, the concentration of HONO has a lower and upper limit for a certain value of NO (Fig. S1(c)). For each preset values of $J(O^1D)$ and NO, we can calculate the average and standard deviation of $P_{unknown}$. As showed in Fig. S1(d), in such a chemical environment at our research site, the errors of $P_{unknown}$ caused by the calculated OH radicals are lower than 1 ppb/h. In the case of low concentration of NO and high value of $J(O^1D)$, the error of $P_{unknown}$ from OH will be restrained significantly. This result shows that it's a good way to reduce the uncertainty of $P_{unknonw}$ by selecting data from 10:00 to 14:00 LT every day.

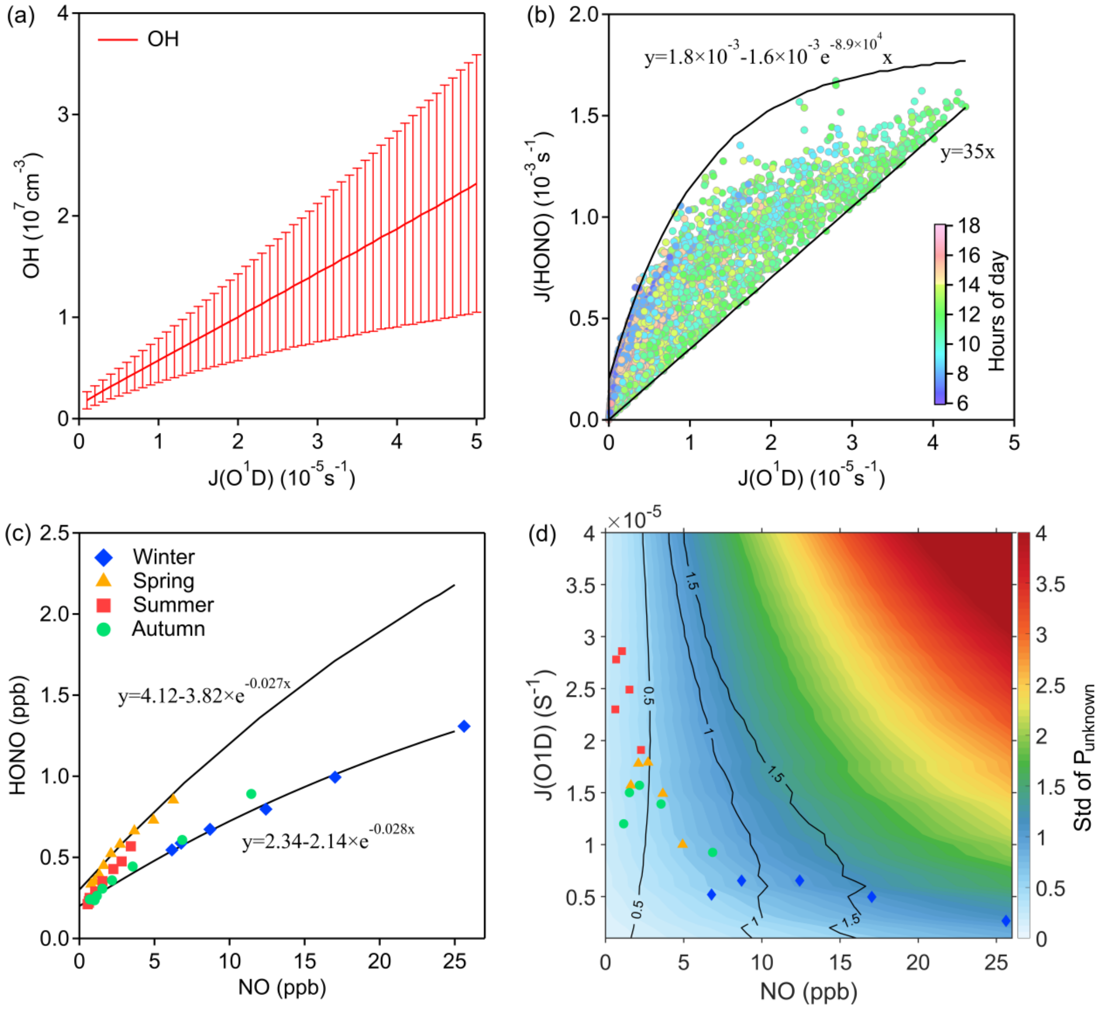

Fig. S1. (a) The average concentration and standard deviation of OH radicals derived from Eq. (2) by changing the values of coefficients **a**, **b**, **c**; (b) the relationship of calculated J(HONO) and J(O^{1}D); (c) the relationship of observed HONO and NO based on diurnal variations (10:00-14:00 LT); (d) the standard deviation of the strength of missing daytime source (Std of $P_{unknown}$) under various values of J(O^{1}D) and NO, and the solid isolines show the ratio of standard deviation to mean value of $P_{unknown}$. The colored and shaped markers in (c) and (d) represent the situations during different seasons.

Table S2. the emission ratios ΔHONO/ΔNO$_x$ in 55 selected fresh plumes, r is the correlation coefficient between ΔHONO and ΔNO$_x$.

Start Time	Duration(min)	△NO/△NO$_x$	r	△HONO/△NO$_x$(%)
11/15/2017 19:50	20	0.88	1.00	0.51
11/15/2017 20:50	30	1.00	0.97	0.42
11/15/2017 21:40	30	1.05	0.91	0.59
11/20/2017 21:50	110	0.91	0.90	0.79
11/21/2017 03:10	70	1.06	0.97	0.33
11/22/2017 05:40	30	1.14	0.93	0.35
11/23/2017 06:00	20	1.10	1.00	0.26
11/23/2017 19:30	110	1.09	0.92	0.67

11/24/2017 01:50	20	1.23	0.94	0.63
11/24/2017 17:20	20	0.91	0.98	0.48
11/28/2017 23:30	40	1.07	0.91	0.82
12/01/2017 01:10	120	1.07	0.91	0.64
12/03/2017 04:40	20	1.00	0.97	0.29
12/03/2017 23:00	30	1.12	0.93	1.91
12/07/2017 01:40	50	1.12	0.96	0.68
12/07/2017 05:40	20	0.85	0.93	0.42
12/07/2017 06:40	20	0.93	0.98	0.63
12/08/2017 19:40	20	1.08	0.99	0.98
12/08/2017 23:30	120	1.10	0.93	0.74
12/09/2017 20:20	120	0.89	0.90	0.74
12/11/2017 04:10	30	1.13	0.92	0.93
12/11/2017 07:10	20	1.13	0.94	0.97
12/17/2017 19:40	120	1.04	0.96	1.02
12/18/2017 03:10	90	1.09	0.94	0.59
12/20/2017 23:50	40	1.15	0.95	0.97
12/21/2017 01:20	40	1.21	0.90	0.98
12/21/2017 03:20	40	1.28	0.95	1.52
12/23/2017 07:10	30	0.96	0.97	1.09
12/23/2017 17:10	60	1.08	0.97	1.11
12/25/2017 02:00	110	1.05	0.91	0.81
12/26/2017 20:20	20	1.05	0.99	0.96
12/28/2017 22:40	100	1.02	0.92	1.29
01/10/2018 22:20	120	1.02	0.95	1.05
01/20/2018 23:50	120	1.20	0.93	1.36
01/21/2018 03:00	70	1.01	0.98	0.66
01/21/2018 19:20	50	1.03	0.98	0.38
01/30/2018 23:00	40	1.09	0.94	0.67
01/31/2018 04:10	70	1.16	0.90	0.67
01/31/2018 18:30	20	0.96	0.96	0.74
03/22/2018 03:30	110	0.87	0.94	0.44
04/10/2018 21:40	110	0.91	0.94	1.02
04/15/2018 20:50	50	0.94	0.97	1.47
04/27/2018 03:10	20	1.03	0.99	0.46
05/12/2018 19:20	30	0.88	0.92	1.21
05/30/2018 02:50	30	0.88	1.00	1.50
07/04/2018 02:20	20	0.91	1.00	0.42
09/28/2018 19:30	20	0.94	0.96	1.37
09/28/2018 21:40	40	0.99	0.98	0.80
09/29/2018 23:40	20	0.92	1.00	0.33
10/11/2018 01:20	120	0.96	0.92	0.65
10/22/2018 21:50	20	0.94	0.99	0.42
10/26/2018 22:50	110	1.07	0.90	0.92

10/27/2018 21:00	30	1.00	0.91	0.63
10/28/2018 00:00	70	0.99	0.91	0.58
11/21/2018 04:10	70	0.95	0.94	0.51

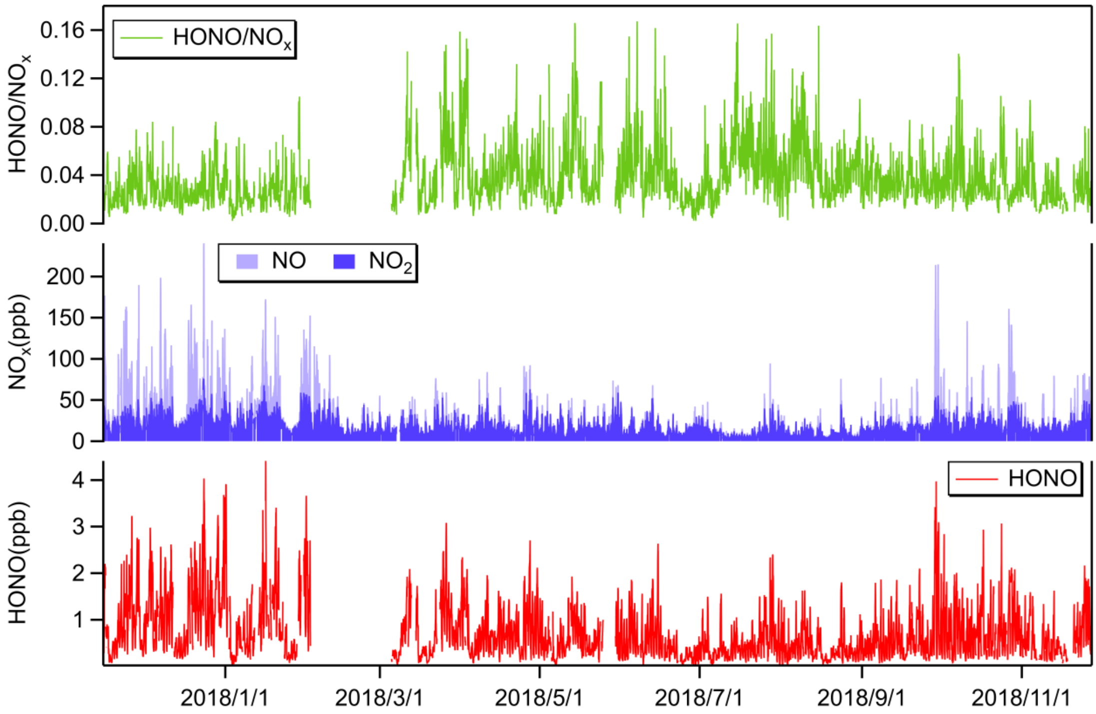

Fig. S2. Time series of HONO, NO, NO_2, $HONO/NO_x$ in Nanjing from November 2017 to November 2017. The data gap is mainly due to the maintenance of the instruments.

When $\frac{\Delta HONO}{\Delta t}$ is approximately equal to zero, usually occurring around noon, the daytime HONO concentration reaches a photo stationary state, so the production rate of HONO from missing source can be calculated by the following equation, deformed by Eq. (10) :

$$HONO_{unknown} = \frac{P_{unknown}}{J(HONO) + k_{HONO+OH}[OH] + \frac{\nu_{HONO}}{H}}$$

As mentioned by Kleffmann et al. (2005) and Lee et al. (2013), the judgment of quasi-steady state can bring great uncertainty, so several stringent conditions are used to selected data: (1) the absolute value of $\frac{\Delta HONO}{\Delta t}$ <0.05 ppb/h; (2) hours around midday (10:00-14:00 LT); (3) rainless and cloudless day (UVB>0.2 W/m^2);

Then we can derive the OH production rate from the missing HONO, which has been found to contribute about 53% of P_{OH}(HONO), showed in Fig. S2, suggesting that it's necessary to consider the unknown source of HONO in models.

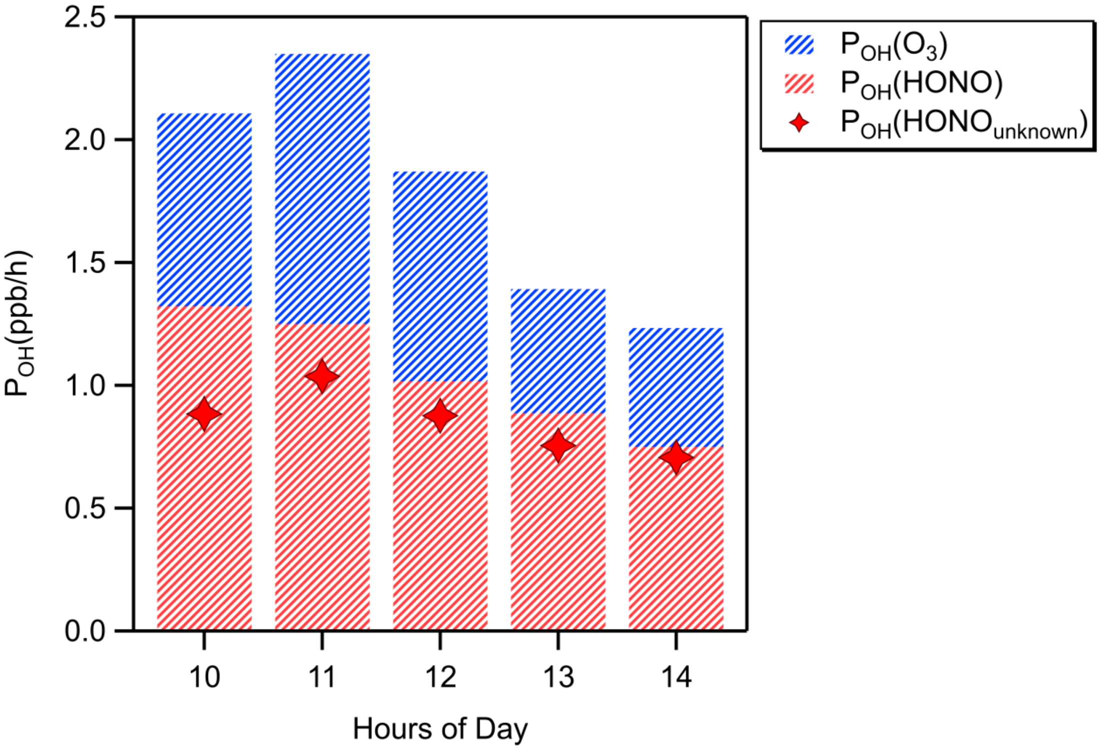

Fig. S3. Averaged OH production rates from photolysis of HONO, missing HONO and O_3 around noon (10:00-14:00 LT), from Nov. 2017 to Nov. 2018.

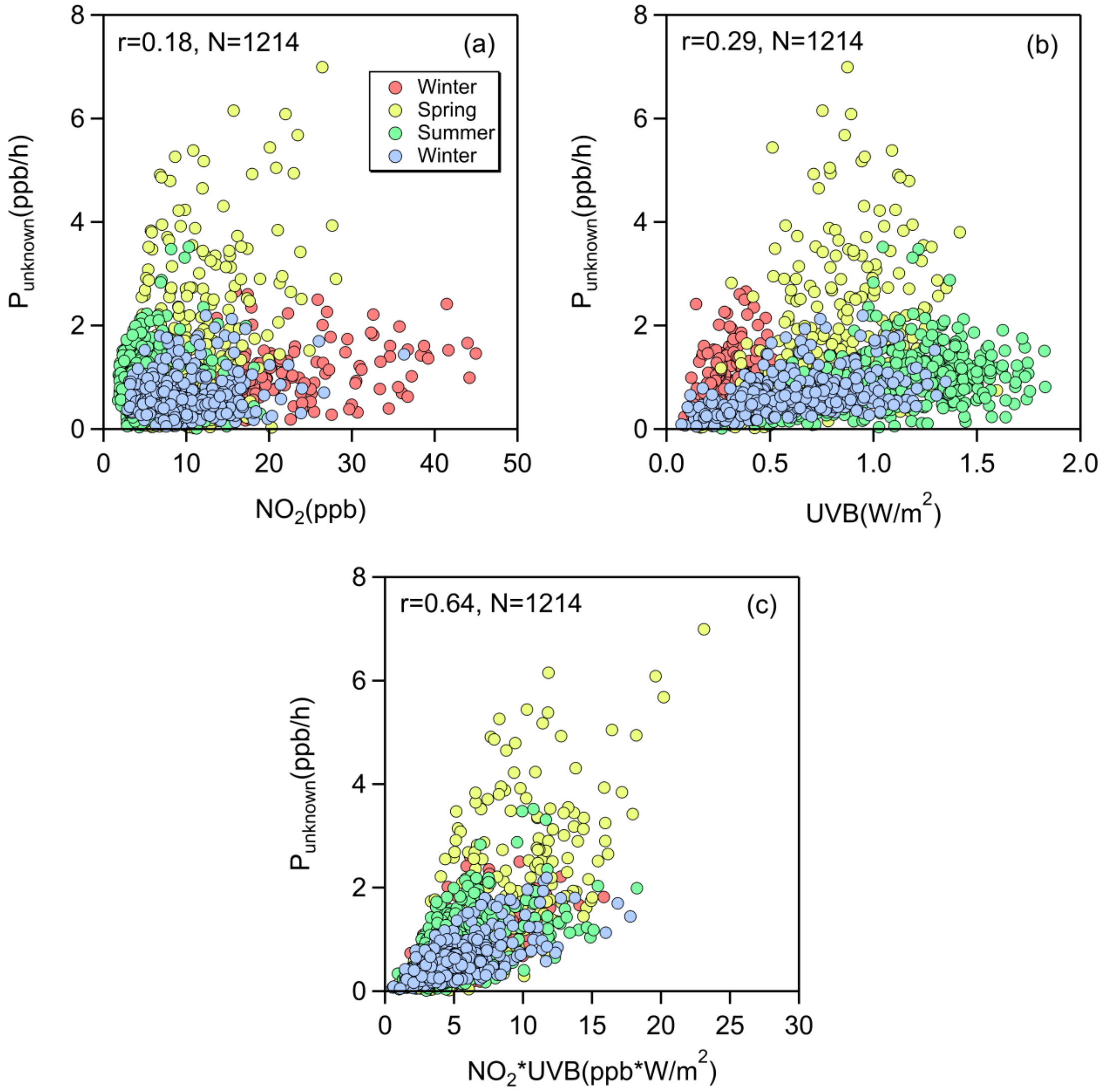

Fig. S4. Correlations between the strength of missing HONO source ($P_{unknown}$) and（a) NO_2, (b) UVB, (c) NO_2*UVB around noon (10:00-14:00 LT), from Nov. 2017 to Nov. 2018. $P_{unknown}$ is better correlated with NO_2*UVB than with NO_2 or UVB alone (p=0.01), perhaps associated with the photo-enhanced converting from NO_2 to HONO.

Reference

Berresheim, H., Plass-Dulmer, C., Elste, T., Mihalopoulos, N., and Rohrer, F.: OH in the coastal boundary layer of Crete during MINOS: Measurements and relationship with ozone photolysis, Atmospheric Chemistry and Physics, 3, 639-649, 10.5194/acp-3-639-2003, 2003.

Brauers, T., Hausmann, M., Bister, A., Kraus, A., and Dorn, H. P.: OH radicals in the boundary layer of the Atlantic Ocean 1. Measurements by long-path laser absorption spectroscopy, J. Geophys. Res.-Atmos., 106, 7399-7414, 10.1029/2000jd900679, 2001.

Holland, F., Aschmutat, U., Hessling, M., Hofzumahaus, A., and Ehhalt, D. H.: Highly time resolved measurements of OH during POPCORN using laser-induced fluorescence spectroscopy, Journal of Atmospheric Chemistry, 31, 205-225, 10.1023/a:1005868520002, 1998.

Holland, F., Hofzumahaus, A., Schafer, R., Kraus, A., and Patz, H. W.: Measurements of OH and HO2 radical concentrations and photolysis frequencies during BERLIOZ, J. Geophys. Res.-Atmos., 108, 22, 10.1029/2001jd001393, 2003.

Kleffmann, J., Gavriloaiei, T., Hofzumahaus, A., Holland, F., Koppmann, R., Rupp, L., Schlosser, E., Siese, M., and Wahner, A.: Daytime formation of nitrous acid: A major source of OH radicals in a forest, Geophysical Research Letters, 32, 4, 10.1029/2005gl022524, 2005.

Lee, B. H., Wood, E. C., Herndon, S. C., Lefer, B. L., Luke, W. T., Brune, W. H., Nelson, D. D., Zahniser, M. S., and Munger, J. W.: Urban measurements of atmospheric nitrous acid: A caveat on the interpretation of the HONO photostationary state, J. Geophys. Res.-Atmos., 118, 12274-12281, 10.1002/2013jd020341, 2013.

Lu, K. D., Rohrer, F., Holland, F., Fuchs, H., Bohn, B., Brauers, T., Chang, C. C., Haseler, R., Hu, M., Kita, K., Kondo, Y., Li, X., Lou, S. R., Nehr, S., Shao, M., Zeng, L. M., Wahner, A., Zhang, Y. H., and Hofzumahaus, A.: Observation and modelling of OH and HO2 concentrations in the Pearl River Delta 2006: a missing OH source in a VOC rich atmosphere, Atmospheric Chemistry and Physics, 12, 1541-1569, 10.5194/acp-12-1541-2012, 2012.

Lu, K. D., Hofzumahaus, A., Holland, F., Bohn, B., Brauers, T., Fuchs, H., Hu, M., Haseler, R., Kita, K., Kondo, Y., Li, X., Lou, S. R., Oebel, A., Shao, M., Zeng, L. M., Wahner, A., Zhu, T., Zhang, Y. H., and Rohrer, F.: Missing OH source in a suburban environment near Beijing: observed and modelled OH and HO2 concentrations in summer 2006, Atmospheric Chemistry and Physics, 13, 1057-1080, 10.5194/acp-13-1057-2013, 2013.

Rohrer, F., and Berresheim, H.: Strong correlation between levels of tropospheric hydroxyl radicals and solar ultraviolet radiation, Nature, 442, 184, 10.1038/nature04924 https://www.nature.com/articles/nature04924#supplementary-information, 2006.

Rohrer, F., Lu, K., Hofzumahaus, A., Bohn, B., Brauers, T., Chang, C.-C., Fuchs, H., Häseler, R., Holland, F., Hu, M., Kita, K., Kondo, Y., Li, X., Lou, S., Oebel, A., Shao, M., Zeng, L., Zhu, T., Zhang, Y., and Wahner, A.: Maximum efficiency in the hydroxyl-radical-based self-cleansing of the troposphere, Nature Geoscience, 7, 559-563, 10.1038/ngeo2199, 2014.

Tan, Z., Fuchs, H., Lu, K., Hofzumahaus, A., Bohn, B., Broch, S., Dong, H., Gomm, S., Haeseler, R., He, L., Holland, F., Li, X., Liu, Y., Lu, S., Rohrer, F., Shao, M., Wang, B., Wang, M., Wu, Y., Zeng, L., Zhang, Y., Wahner, A., and Zhang, Y.: Radical chemistry at a rural site (Wangdu) in the North China Plain: observation and model calculations of OH, HO2 and RO2 radicals, Atmospheric Chemistry and Physics, 17, 663-690, 10.5194/acp-17-663-2017, 2017.

Tan, Z., Rohrer, F., Lu, K., Ma, X., Bohn, B., Broch, S., Dong, H., Fuchs, H., Gkatzelis, G. I., Hofzumahaus, A., Holland, F., Li, X., Liu, Y., Liu, Y., Novelli, A., Shao, M., Wang, H., Wu, Y., Zeng, L., Hu, M., Kiendler-Scharr, A., Wahner, A., and Zhang, Y.: Wintertime photochemistry in Beijing: observations of ROx radical concentrations in the North China Plain during the BEST-ONE campaign, Atmospheric Chemistry and Physics, 18, 12391-12411, 10.5194/acp-18-12391-2018, 2018.